Thermal Convection in a Completely Confined Fluid Layer

W. T. MITCHELL and J. A. QUINN

University of Illinois, Urbana, Illinois

Experimental observations are reported on convective motion in a laterally confined fluid layer heated from below. Measurements extend over a wide range of Rayleigh numbers which encompass several flow regimes, including remarkably stable periodic flows. The conditions necessary for the oscillatory motion as well as the qualitative nature of the flow have been explored.

Take a cylinder with radius equal to height; place the cylinder (axis vertical) between two heated, horizontal plates, the lower of which is maintained at a temperature several degrees higher than the upper; insert a sensitive thermocouple into the gas space enclosed by the cylindrical wall and the flat plates, and monitor the signal coming from the heated air. The magnitude of the signal will be proportional to the temperature at the tip of the thermocouple; moreover, with proper sensitivity, it will be noted that the signal fluctuates about some mean value. On closer examination the fluctuating signal proves to be a regular oscillation with a period of several seconds per cycle; with constant plate temperatures the oscillation is remarkably stable. This is one of the more striking manifestations of buoyancy-driven convection within a completely confined fluid layer heated from below. In this paper we detail experiments and observations which we have made on high Rayleigh number flows (Rayleigh numbers well beyond the onset of motion) in laterally confined gas layers.

BUOYANCY-DRIVEN CONVECTION

Flow in the heated layer considered here is a special case of the general problem of convective instability (*13*) wherein sustained fluid motion results from gravitational forces acting on an unstable density gradient. In almost all previous investigations of natural convection in horizontal layers, the system examined has been that of a laterally infinite layer, uniformly heated from below. This was the model first analyzed theoretically by Rayleigh (*11*) with subsequent refinements of the theory by Jeffreys and others (*4, 5*), the work of Pellew and Southwell (*10*) being of particular significance. The result of these analyses is the prediction of the conditions which govern the onset of the convective motion; because the theory is derived from the linearized equations of motion, these predictions constitute the so-called *linear stability theory*—as apposed to a nonlinear theory which treats the developed flow. Chandrasekhar presents a comprehensive treatment of the linear theory in his monograph (*1*) as well as a review of prior work on the infinite layer.

PREDICTIONS OF LINEAR STABILITY THEORY

In the context of the present study, the principal results of linear theory for the unbounded layer are:

1. There is a fixed value of the Rayleigh number

$$N_{Ra} = N_{Gr}N_{Pr} = \frac{g\alpha\Delta T h^3}{\kappa\nu}$$

below which the layer is stable and above which instability, that is, motion sets in. This single dimensionless group characterizes the system, and its numerical value at the onset of flow depends on both the thermal and dynamical conditions at the two bounding planes. (A critical value of 1,708 is obtained for the case of rigid, constant temperatures surfaces.)

2. The transverse structure of the resulting flow is that of ordered polygonal cells, the lateral walls of which are surfaces of symmetry. For rigid, constant-temperature, bounding surfaces the ratio of cell spacing to layer depth is approximately three. (Experimentally, it is observed that the cells are usually hexagons, frequently called Bénard cells.)

3. At the point at which motion first appears, the state of marginal stability, the flow can be either stationary (time independent) or it can oscillate with a definite characteristic frequency. Pellew and Southwell proved that for the unbounded layer the "principle of the exchange of stabilities" is valid. This principle states that whenever sustained motion is possible it must be aperiodic (or stationary) and oscillatory flows are precluded.

EXTENSIONS TO THE COMPLETELY CONFINED LAYER

For the completely confined fluid layer, it is assumed that the fluid is contained between two horizontal planes and a vertical cylinder of arbitrary cross section. Apparently there has been little theoretical work done on this case; Pellew and Southwell and Ostrach and Pnueli (*8*) have considered certain aspects of the linear analysis but no comprehensive treatment of the stability problem exists at this time.

A complicating factor which appears in the confined problem is the thermal boundary condition at the wall. Whereas the cell walls of the unbounded case are no-flux surfaces, the rigid walls may be insulating or conducting. Moreover, the linear analysis can be solved (by the usual separation technique) only for the situation where the temperature perturbation on the wall is zero, that is, the initial constant temperature gradient on the wall is not disturbed by the flow (*10*). This limitation exists because in performing the stability analysis, the linearized equations of energy and motion are combined, eliminating all but one dependent variable which may be either the vertical component of velocity w or the temperature T. The variables of the combined equation (the equations in w or T are identical) are assumed to be separable such that the velocity (or temperature) can be expressed as a product of three functions: one a function of t alone, one a function of z alone, and the remaining one, the planform function, dependent only on x and y, the coordinates in the horizontal plane. However, the variables can be

W. T. Mitchell is with Celanese Chemical Corporation, Corpus Christi, Texas.

separated if, and only if, the boundary conditions at the wall are identical on both w and T. This restriction is satisfied for the infinite layer since the cell walls are surfaces of symmetry over which the normal derivative of both w and T vanishes; for rigid walls, w is zero and this implies that for separation the temperature perturbation on the wall must also be zero. Experimentally, a temperature distribution of this type can be closely approximated by using massive walls with a thermal conductivity much higher than that of the enclosed fluid.

Pellew and Southwell solved the separated equations for a circular wall of radius R. Their solution for the vertical velocity is of the form

$$w = A_n \cos(n\theta + \alpha_n) J_n(kr) \tag{1}$$

with A_n and α_n arbitrary constants and

$$k^2 = a^2/h^2 \tag{2}$$

where h is the depth of the fluid layer and a represents the separation constant or wave number (*1*). Furthermore, since the velocity must go to zero at the wall

$$J_n(kR) = 0 \tag{3}$$

This last condition fixes a, which in turn determines the critical Rayleigh number (*10*).

As pointed out by Ostrach and Pnueli, certain values listed by Pellew and Southwell for aR/h violate the continuity equation. Since there is no net axial flow, continuity is satisfied by

$$\int_0^{2\pi} \int_0^R wrdrd\theta = 0 \tag{4}$$

with Equations (3) and (4) being incompatible for $n = 0$, the condition of radial symmetry. The fact that $n = 0$ is not a solution gives the somewhat surprising result that no axisymmetric flows are allowed (by linear theory). This point is discussed further in a later section.

The question of oscillatory instability, or overstability, in the bounded layer was first considered by Yih (*16*) for the case of a fluid contained between constant temperature horizontal planes and an insulated cylindrical wall. Yih proved the principle of the exchange of stabilities for this case. More recently, Sani and Scriven (*13*) have shown that under very general boundary conditions on both the horizontal and vertical surfaces, enclosed systems such as those considered here cannot exhibit overstability. Again it should be emphasized that this is a conclusion from small disturbance theory, and it may not be valid for the developed convective flow at the high Rayleigh numbers studied in the present experiments.

PREVIOUS EXPERIMENTAL INVESTIGATIONS

In general, there is little experimental information on the temperature field and convective flow in heated, unbounded fluid layers for Rayleigh numbers greater than a few thousand. For bounded layers, the authors are not aware of any published results on flow conditions at the Rayleigh numbers (10^4 to 10^5) and radius-to-layer thickness ratio (0.5 to 2) covered here. Chandrasekhar (*1*) describes the usual experimental techniques for detecting the onset of motion as well as summarizing the major experimental findings for the infinite layer. In the heat transfer literature, O'Toole and Silveston (*9*) have reviewed (and correlated) heat transfer coefficients reported by several authors for Rayleigh numbers as high as 10^9.

Schmidt and Saunders (*14*) observed that beyond the onset of motion, an ordered, cellular flow persisted up to Rayleigh numbers of approximately 50,000. At this value the flow became irregular, with the ordered motion replaced by a random, turbulent flow. Malkus (*6*) extended these results and he reported six discrete flow transitions between Rayleigh numbers of 1,700 and 10^6, with the higher transitions being from one mode of turbulent convection to another. He noted a transition at $N_{Ra} \sim 55{,}000$ which he associates with the transition determined by Schmidt and Saunders; however, he measured a still lower, though less distinct, transition in the range of 10,000 to 30,000. It is at this lower transition that Malkus first observed turbulent convection.

Because of his experimental arrangement, Malkus was concerned with the effect of vertical boundaries on the heat transport and velocity field in the convecting layer. The fluids which he studied (water and acetone) were confined between two horizontal plates and a cylindrical wall 10 cm. in diameter, with the plate spacing ranging from 0.05 to 8.0 in. To measure the effect of the walls, in one experiment he inserted a thin-walled vertical cylinder, 7 cm. in diameter, concentric with the outer wall. He notes: "The reduction in heat transport was less than 1%, despite a marked reduction in the horizontal fluctuations of the fluid." From this he concluded that the heat transport is independent of the horizontal motion and, therefore, unaffected by the vertical walls.

SCOPE OF THE PRESENT EXPERIMENTS

The experimental work described in this paper was undertaken to explore the various convective phenomena which occur in bounded fluid layers heated from below. Mean and fluctuating temperatures in several cylindrical configurations have been measured; also, flow visualization techniques have been used to examine the structure of the convective flow. It is anticipated that these observations will aid in the formulation of nonlinear theories of buoyancy-driven convective transport.

EXPERIMENTAL ARRANGEMENTS

Several types of measurements were made with many different experimental arrangements. In this section the basic features of the apparatus and procedure are given.

Horizontal Plates

The basic experimental setup is shown in Figure 1. The heating surfaces in most of the experiments were 12 in. by 12 in. by 5/8 in., twelve-pass brass heat exchangers, the facing surfaces of which were carefully milled flats. Plate spacing was maintained with micrometer heads mounted at the four corners of the upper plate. Water flow rates were such that the maximum temperature difference across the plate surface was less than 1°C. The plates were stacked with lateral gradients opposed with the result that the temperature difference over the test section was practically constant. For certain measurements, the entire outer surface of the plates and the gap between the plates was blanketed with a heavy layer of insulation. Water temperature to the plates could be controlled and maintained within 0.1°C.

Cylindrical Enclosures

The fluid layer was confined laterally with a cylindrical wall made of 1/4-in.-thick Plexiglas. Walls of brass and of heavy paper were also used in a limited number of tests. Horizontal openings were drilled into the side of those cells

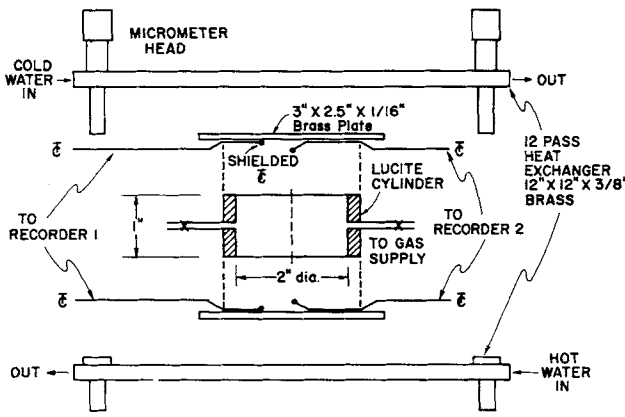

Fig. 1. Exploded side view of equipment showing cell with thermocouples.

used for gases other than air. Gas was introduced through these ports and the enclosure was made gas-tight by coating the contact surfaces of the cylinder and plates with a thin layer of stopcock grease.

Thermocouples

Plate temperatures were measured with thermocouples attached to but electrically insulated from the brass surfaces. The electrical insulation consisted of a thin layer of epoxy cement; also, the soldered junctions of the thermocouple wire (30-gauge copper-constantan) were covered with small pieces of tape to minimize radiation errors. Temperature differences were obtained directly by opposing the thermocouples on the two plates.

Temperatures in the gas space were monitored with highly sensitive thermocouples made from 1-mil copper-constantan wire. Junctions were fabricated by a single twist of the fine wire followed by fusion of the metals in a flame.

Recording Equipment

Temperatures were amplified and recorded with several instruments, principally a 1-mv. chart recorder (Sargent model SR). At various times signals were also displayed on a vacuum tube voltmeter (Hewlett-Packard model 425 A) and a multichannel recorder (Sanborn series 150). The amplitude and frequency of the thermocouple signals were well within the resolving power of these instruments and the temperature records are relatively undistorted.

Flow Visualization

For visualizing the flow, the brass plates were replaced by transparent surfaces. The lower heating plate was a 12 in. by 12 in. square of electrically conducting glass (Corning Glass Works, code 7740, 20 ohms/square) which was heated electrically. The glass had ½-in. silvered connection strips on opposite sides to provide a uniform conduction field. The upper plate was an 8 in. by 8 in., single-pass Plexiglas heat exchanger with a ¼-in. flow gap through which cooling water was circulated.

A small quantity of cigar smoke introduced through the side opening on the cylindrical wall rendered the flow visible, with the best contrast obtained by placing dull black paper beneath the heating glass and illuminating the system horizontally. Both still and motion pictures were taken from above.

OBSERVATIONS

Oscillations in the Temperature Field

As a first method of detecting flow transitions, a thermocouple was placed in the heated gas space enclosed by the horizontal plates and the cylindrical wall. It was anticipated that abrupt changes in gas temperature would coincide with changes in the flow pattern. Subsequent experiments (discussed later) showed that the presence of the thermocouples in the gas did not drastically alter fluid motion. It should be noted that these measurements provide information on time-dependent flows only.

In certain cell configurations, as the plate temperature difference, and therefore the Rayleigh number, was increased well beyond the point at which motion first set in, the gas temperature appeared to oscillate with a well-defined frequency. Further examination showed that the fluctuating signal was characteristic of a regular oscillatory mode of convection which, once established, was remarkably stable and which persisted over a range of Rayleigh numbers.

Typical temperature patterns are shown in Figure 2. The four sample sequences have been taken directly from chart recordings of the thermocouple response. The first trace shows the onset of an oscillating flow. Prior to the onset, the lower plate temperature was slowly increased; at some critical Rayleigh number, the oscillation set in spontaneously as shown. If the plate temperatures were then held constant, the oscillation would continue with constant amplitude and frequency. With constant external conditions, there was no indication that the oscillation was decaying; in fact, some patterns were maintained over periods as long as 24 hr. with no noticeable change. In observing the temperature oscillations the thermocouples were positioned in various locations throughout the gas space. Though the amplitude of the signal varied from point to point, the frequency was independent of thermocouple position.

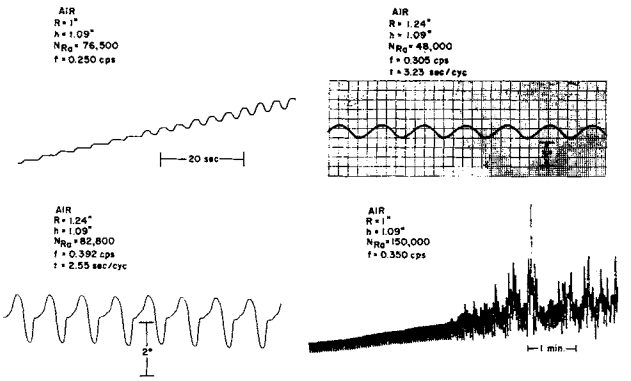

Fig. 2. Typical temperature oscillations: onset of oscillation, fully developed sinusoidal trace, fully developed complex signal, and transition from regular to random signal.

The second trace of Figure 2 shows a simple, sine wave type of fluctuation, whereas the next pattern is an example of a more complex signal. Though the frequency of the oscillation was characteristic of the cylinder size and N_{Ra}, the amplitude and wave form varied throughout the gas volume. Many signals appeared to be composed of a fundamental frequency with higher harmonics superimposed. As would be expected, the oscillatory transition was not highly reproducible and it also exhibited metastability, that is, the transition point was influenced by the rate of change of the plate temperatures. With rapid heating of the lower plate, the transition was delayed and oscillation first appeared at a higher temperature than occurred with gradual heating. Also, the flow regime was sensitive to thermal shocks and to mechanical disturbances. On occasion, an oscillation was induced by jarring a system which was in a nonoscillatory state but at a temperature cose to the transition.

The last temperature record shown in Figure 2 represents a transition from an ordered to a random fluctuation. Such transitions were always observed as the overall temperature difference was increased beyond the oscillatory region. In summary, the following sequence was displayed as ΔT was increased: first the temperature was relatively constant; then, depending on the heating rate and external disturbances, a regular oscillation set in which persisted, with slight change in amplitude and frequency, over an extended temperature range; on further increase, the signal became irregular, indicating that some turbulence was present. The sequence was reversible; however, the transition temperatures on cooling were usually shifted from the heating values; with very slowly varying temperatures the heating and cooling curves would probably coincide.

Rectangular enclosures of approximately the same dimensions as the cylinders were also examined. Though oscillations were detected in several cells, it proved much more difficult to establish oscillations in these cells and the data were somewhat inconsistent with a general lack of reproducibility. A hexagonal cell geometrically similar to that predicted by linear theory for the unbounded layer was studied in the same Rayleigh number range as the circular cells. The behavior was similar to that of the rectangular cells.

To confirm that the oscillations were not the result of some spurious feature of the temperature detecting or heating techniques, several auxiliary experiments were performed. In one test, twin cells with identical dimensions were placed side-by-side with thermocouples in each. Due to the metastable nature of the oscillation, it was possible to induce an oscillation in one cell (by a pressure disturbance) while a steady flow remained in the matching cell. This would seem to indicate that the oscillation is not triggered by a feed-back mechanism acting between the heating surface and the convecting gas; nor is the oscillation brought on by a disturbance in the plate temperature, for if this were the case one would expect the onset to occur simultaneously in both cells. With increasing temperature, an oscillation was eventually established in the second cell and the frequencies of the two signals were identical.

As a demonstration that the presence of the thermocouples did not influence the phenomenon, the average pressure in an oscillating cell was measured. This was accomplished by connecting a strain-gauge differential pressure transducer (bidirectional strain gauge, ± 0.3 lb./sq. in. gauge range, model 283 TC, Statham Instruments, Inc.) between the two openings drilled into the side of a cell (Figure 1). With the cell sealed to the plates and with all thermocouples removed, it was observed that the average gas pressure oscillated with precisely the same frequency as measured with a thermocouple in the unsealed cell (that is, with side ports open and without sealing grease at the contact surfaces of the cylinder and plates). The amplitude of the pressure oscillation was 3×10^{-3} lb./sq. in. This corresponds to an *average* temperature oscillation of the order of 0.06°C., which in turn was approximately 5% of the point temperature oscillation. The oscillation in average temperature indicates that the heat flux to and from the cell was also undergoing a periodic fluctuation.

Rayleigh Number Dependence

A functional relationship among the various quantities involved can be obtained by reducing the boundary conditions and the equations governing the convection (the equations of motion and energy and the continuity equation) to a dimensionless form. By making the Boussinesq approximation (*1*), three groups appear: the Rayleigh number, the Prandtl number, and the ratio of plate spacing to cell radius (h/R). An effect due to the Prandtl number alone cannot be discerned in the present observations, since all the gases studied have substantially the same Prandtl number.

For fixed cell dimensions the Rayleigh number can be varied by changing plate temperatures or gas properties. By using several different gases in the same cell (1.0-in. radius by 1.1-in. height) the following data were obtained, with N_{Ra} and ΔT representing conditions at the onset of the oscillation

Gas	N_{Ra}	ΔT, °C.
Methane	50,000	27
Air	43,000	19
Carbon dioxide	47,000	5
Ethane	56,000	5

By considering the approximate nature of the data, the fact that all values of N_{Ra} are of the same order would seem to indicate that there is a critical value of N_{Ra} at which the transition occurs. This critical Rayleigh number depends on cell size but for all cylinders tested (listed in Table 1) the transition fell in the range of 20,000 to 200,000. The higher transition, from the regular oscillation to an irregular, random flow, took place, again depending on cell dimensions, from about 35,000 to well over 200,000.

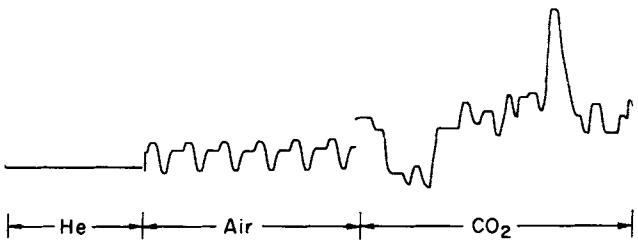

Fig. 3. Helium, air, and carbon dioxide, alternately, in the R = 1.24 in., h = 1.09 in. cell with ΔT = 20.0°C. N_{Ra} = 500 for helium, 46,000 for air, and 136,000 for carbon dioxide.

The flow sequence is readily apparent in Figure 3 which shows the temperature response in a cell (1.25-in. radius by 1.1-in. height) with fixed ΔT (20°C.) as helium, air, and carbon dioxide were alternately placed in the cell. (The time axis in Figure 3 is not continuous, that is, the recorder was stopped while gas was flushed through the cell.) At this ΔT the Rayleigh numbers for the three gases were 500, 46,000, and 136,000, respectively. For helium, the value was well below the first transition and the gas was stable with no convective flow. Air was within the oscillatory region and with carbon dioxide the flow was turbulent.

Frequency Measurements

The period of the temperature oscillation is not uniquely determined by the Rayleigh number and cell dimensions. In several cells there appeared to be more than one oscillatory state, each characterized by a different frequency. However, in all cases where multiple states were encountered the total spread in frequencies was small—with one exception. (The exceptional case of h/R equal to one is discussed below.) Typical behavior is shown in Figure 4 where frequency is plotted as a function of N_{Ra}. The three lines correspond to three different states. The frequency was caused to change discontinuously from one state to another by perturbing the flow with a pressure surge. (A surge was generated by suddenly compressing a piece of flexible tubing connected to one of the side ports, the other port being open to the atmosphere.)

In a given state, the frequency varied linearly with ΔT (or N_{Ra}) and, as can be seen in Figure 4, the ΔT dependency was nearly identical in each of the states. The maximum number of states detected in any cell was seven with a total frequency variation among the various states of less than 10%. As a further test, experiments

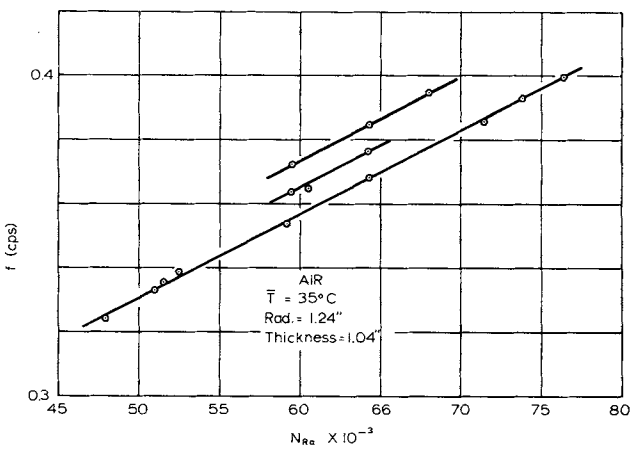

Fig. 4. Frequency vs. N_{Ra} at constant average temperature for three oscillatory states.

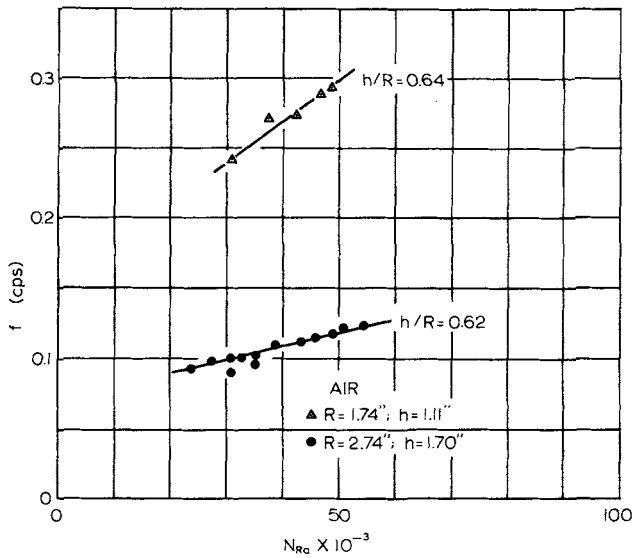

Fig. 5. A comparison of frequencies in two cells with approximately the same *h/R*.

were performed in which the ΔT was first increased to the turbulent region with subsequent gradual cooling into an oscillatory state. No particular frequency was preferred and any of the possible states appeared with equal probability. Evidently, the states are nearly equivalent in energy. With great care it might be possible to identify one form as the ground state for a particular N_{Ra}; however, we were unable to detect such a state.

Frequency variation between enclosures of different dimensions is exemplified by the data of Figure 5. The upper points were obtained in a cell of 1.74-in. radius by 1.11-in. height, while the lower curve was measured for a cell of 2.74-in. radius by 1.70-in. height. Even though the cells were geometrically similar (h/R of 0.64 vs. 0.62), the frequencies differed by a factor of two to three. These same results, along with all frequency measurements obtained with circular cells, are plotted in dimensionless form in Figure 6. The variables used in transforming the frequency to dimensionless form were selected somewhat arbitrarily. Obviously, some parameter with units of time is needed; either ν or κ suffice and, since for all gases studied the Prandtl number is near unity, both yield equivalent results. The selection of a length parameter is further discussed below. (The factor of π is, of course, superfluous; it was incorporated with the idea that the circulation loop within a cell is approximately πh in length.)

Depicted as in Figure 6 (see Table 1 for all experimental conditions) the data are separated into two distinct groups, one curve for $h/R < 1$ and the lower curve for

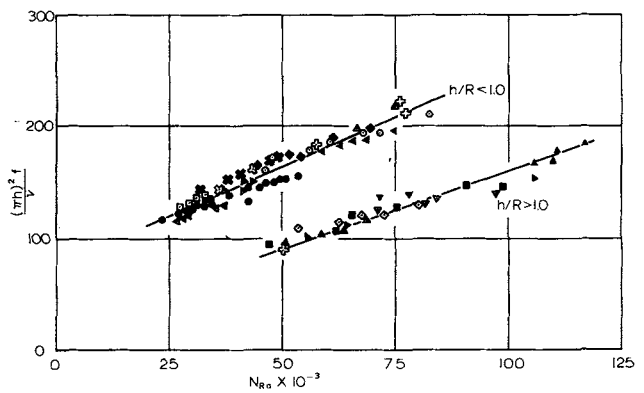

Fig. 6. Frequency data on all cylinders examined. Experimental conditions listed in Table 1.

Table 1. Experimental Conditions for Data Shown in Figure 6

SYMBOL	RUN	GAS	R (in)	h (in)	FREQUENCY RANGE (cps)	ΔT RANGE (°C)
⊙	1	AIR	1.24	1.09	0.305–0.392	17.3–33.7
⊡	2	AIR	1.24	0.88	0.405–0.444	26.9–32.5
▽	3	AIR	1.24	1.48	0.130–0.145	12.2–17.0
✣	4	AIR	1.24	1.19	0.147–0.319	17.9–21.1
△	5	AIR	1.24	1.27	0.139–0.315	14.5–22.3
✚	6	AIR	1.24	1.24	0.328–0.341	25.2–26.2
⊠	7	AIR	1.24	0.90	0.433–0.502	32.5–42.0
●	8	AIR	2.74	1.70	0.090–0.123	2.7–6.2
■	9	AIR	1.00	1.13	0.175–0.299	19.8–52.5
▼	10	AIR	1.00	1.15	0.228–0.235	27.3–30.0
✖	11	AIR	1.49	1.11	0.265–0.325	13.5–21.4
▷	12	AIR	1.74	1.11	0.241–0.292	13.3–21.4
◁	13	AIR	1.49	0.89	0.347–0.394	23.2–36.0
▲	14	AIR	1.00	1.62	0.150–0.172	14.2–18.2
◇	15	METHANE	1.00	1.11	0.220–0.270	28.7–42.0
▶	16	ETHANE	1.00	1.11	0.089–0.136	4.9–9.3
◆	17	METHANE	1.24	1.09	0.347–0.422	23.3–35.9
◀	18	ETHANE	1.24	1.09	0.159–0.175	5.3–6.7

$h/R > 1$; for $h/R = 1$ the results fall randomly into either group. Besides normal experimental error, some of the apparent scatter among the points is due to the variation between states referred to earlier. It should be added that in measuring complicated wave forms the period was always taken as that of the smallest repeating unit.

Flow Patterns

By injecting smoke into a transparent cell, it was possible to observe certain features of the convective flow. These observations were hampered by serious shortcomings inherent in the technique. First, the smoke perturbed the system; second, the smoke was dispersed rapidly by the convective motion leaving only a short time in which contrasts and therefore flow patterns could be observed; third, the aerosol which comprises the smoke may have affected the motion, although we have no evidence that this occurred. Subject to these limitations, only gross details could be discerned. The two most significant observations were: in the range of N_{Ra} immediately preceding and following the oscillatory transition, only four basic flow patterns or modes were detected; the periodic temperature signal was generated by a spiraling motion of the principal flow axes.

In Figure 7 we have sketched the directions of flow for the four basic modes. The arrows in the plan view indicate the prevailing currents as seen from above; near the lower, heated surface flow is in the reverse direction. The dotted lines represent the axes about which the flow rotates; they also separate regions of up- and down-flow. The accompanying side views show the general direction of circulation in selected vertical planes. Note that the first mode differs from the other three in as much as the circulation loop in mode 1 is over the cell diameter, whereas for 2, 3, and 4 the loop closes within the radius of the cell. On this basis we further classify the flows into type A (flow extends over diameter, mode 1) and type B (flow limited to radius of cell, modes 2, 3, and 4). Type A flow was observed only in cells for which $h/R > 1$ and type B flow only in cells with $h/R < 1$. At h/R equal to one the first mode was most frequently seen, though on a few occasions we detected either mode 2 or 4 (in general, it was difficult to distinguish between modes 2 and 4).

To clarify further the flow patterns horizontal temperature profiles were measured along a diameter in the gas space (nontransparent cell). A special cooling plate was constructed with a sliding bar fitted into a slot milled into the upper plate. In position, the surface of the bar was flush with the plate with good metal-to-metal contact

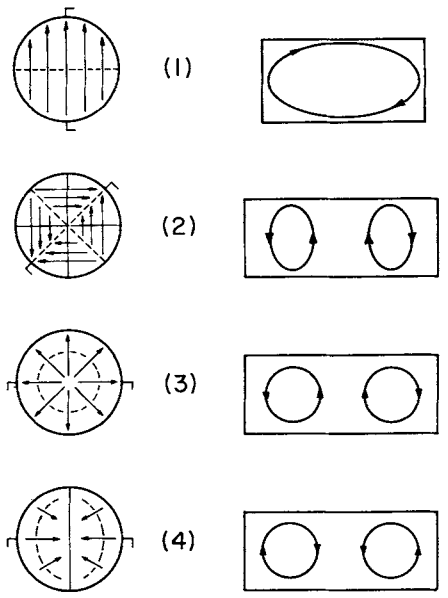

Fig. 7. The four basic modes observed with the smoke technique. The plan view shows the flow lines as seen from above; the cross secton indicates the circulation path.

between the bar and plate. Thermocouples were attached to the underside of the bar so that they extended from ⅛ to ⅜ in. into the gas space with the leads brought out through a groove on the back of the strip. In operation, a cell was positioned with the strip along the cell diameter; the strip (longer than the diameter) was then moved across the cell with a calibrated screw drive. The slide was moved discontinuously, with ample time between moves to allow the slide to attain the proper steady state temperature.

The temperature measurements confirmed certain aspects of the flow established with the smoke patterns. First, the temperature profile just prior to the onset of oscillation was approximately the same as the *mean* profile following the onset—the oscillation did not alter the basic flow. Second, traversing the cell showed that the frequency of the oscillation was independent of position; however, the amplitude, wave form, and phase angle were functions of position. Third, the temperature profiles were of two types depending on the value of h/R. For $h/R < 1$ the profiles were roughly symmetrical about the cell center, while for $h/R > 1$ the profiles were asymmetrical. Both forms were noted in cells with h/R equal to one.

The symmetry of the profiles substantiates the earlier classification of the flows into types A and B. A sample profile corresponding to either mode 2 or 3 is shown in Figure 8. Profiles representative of the other modes were also measured, though in many cases the interpretation was ambiguous, since the orientation of the profile relative to the planes of symmetry was not known.

Of the four observed patterns, two are similar to the predictions of linear theory for a circular cell with conducting walls. The roots of Equation (3) represent allowable values of (aR/h) which in turn determine the transverse structure of the flow when inserted into Equation (1). Each successive root yields a possible flow pattern or mode. By Rayleigh's membrane analogy (*10*), the planform of the flow may be associated with the planform of the displacement of a uniform membrane with the cell wall as a boundary and vibrating freely in a normal mode. [Several of the modes are pictured in Rayleigh's *Theory of Sound* (*12*).] Modes 1 and 2 are equivalent to the lowest vibratory modes consistent with the continuity restriction, Equation (4). Mode 3 is similar to the next highest mode of the vibrating membrane; however, since it is axisymmetric it contradicts the restriction discussed following Equation (4). Mode 4 is, apparently, not predicted by linear theory. In light of the large values of N_{Ra} and the fact that the cell walls of the experiment are more nearly insulating, close correspondence between observation and linear theory is somewhat illusory. The point to be made is that the observed flows did possess a certain order and symmetry, not entirely unlike the simple patterns predicted from a first-order theory.

One last comparison between linear theory and observation is the separation of the flows on the basis of (h/R). If one considers the first transition, that is, the point at which flow commences, the mode which is established can be calculated for any value of (h/R). The procedure is as follows: each mode is characterized by a particular value of (aR/h)—the successive roots of Equation (3); for a fixed (h/R) one determines from a plot of N_{Ra} vs. wave number a (*10*) the value of N_{Ra} which obtains for each of the modes; the mode corresponding to the smallest value of N_{Ra} will be the preferred one. In this manner it can be shown (7) that for (h/R) equal to or greater than 0.82 the motion will set in via mode one. Higher modes are preferred for smaller values of (h/R) and, as (h/R) becomes smaller, the spacing (in N_{Ra}) between modes becomes smaller. Our classification of the observed flows into types A and B is a separation between patterns similar to mode one (type A) and those similar to the higher modes (type B). Experimentally, the separation occurs at (h/R) near one rather than 0.82; however, by considering the gross differences between phenomenon and theory the agreement is impressive. Furthermore, the fact that the higher modes are so closely spaced in terms of their critical Rayleigh number may explain why the flows were divided essentially into two parts with no major splitting, in any of the observations, among the higher modes.

In watching the transition from a steady to an oscillating flow with the smoke technique, the first evidence of change appeared as a slight undulating motion at certain points in the fluid. These undulations grew in size and developed a rhythmic movement as adjacent flow lines moved in unison. The wavy smoke lines were actually three-dimensional spirals rotating about the axes of the suboscillatory flow. As with the turning of a screw, rotation of the spirals gave the illusion of translation along the axis.

A model of the spiraling flow, patterned after the oscillating motion observed with modes 1 and 4, is shown in Figure 9. The continuous line, which represents the axis in the oscillatory flow, has been wound around a cylinder

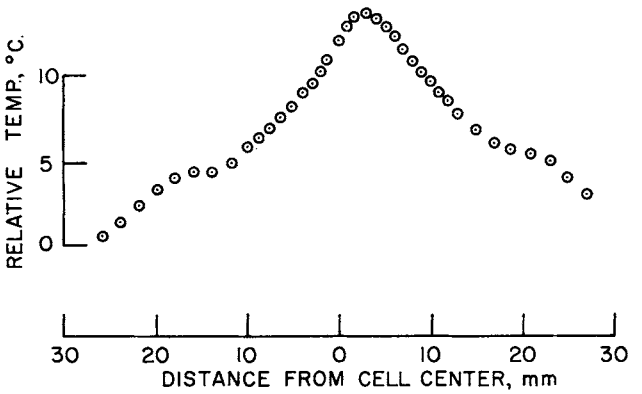

Fig. 8. Sample horizontal temperature profile measured with traversing thermocouple. Experimental conditions: ΔT = 23°C., R = 1.24 in., h = 1.09 in.

lying in the direction of the original axis. The comparable model for mode 3 is depicted in Figure 10; a model for the oscillating streamlines in mode 2 (not shown) would be a line wound on the surface of a cone. The actual spirals for the straight cylinders of modes 1, 2, and 4 had approximately two to three complete turns and the spiral on the torus of mode 3 had four to five complete turns.

In terms of this model, the temperature is constant along a spiral. Rotation of the cylinder gives rise to a periodic temperature at a fixed point such as the arrowhead in Figure 9. The lower two traces in this figure show one-quarter and one-half rotation; a full rotation returns the dot to its original position. Clearly, one revolution corresponds to a complete cycle in the temperature oscillation. From motion pictures of the smoke patterns it was definitely established that the period of the temperature oscillation agreed exactly with the period of the spiraling motion.

Oscillatory motion superimposed on mode 3 is illustrated in the upper photograph of Figure 11. The starlike configuration is the spiral idealized in Figure 10. This photograph is typical of the smoke traces; note that as opposed to the regularity and precision of the models previously described, the symmetry of the actual flows was far from perfect. The accompanying photograph of Figure 11 shows a smoke pattern in mode 4 just prior to the onset of an oscillation. At the onset, the line which bisects the cell developed a waviness characteristic of the spiraling motion.

All oscillating flows grew out of the basic configurations previously described. However, the features which distinguished the basic flow were rapidly blurred as the Rayleigh number was increased beyond the transition point. The accompanying temperature signal reflected the increasing complexity of the motion. Near the onset, the temperature trace was a regular sine wave and with increasing Rayleigh number it became more complex. Perhaps not surprisingly, a regularity frequently persisted in the temperature recording long after any order could be seen in the smoke patterns.

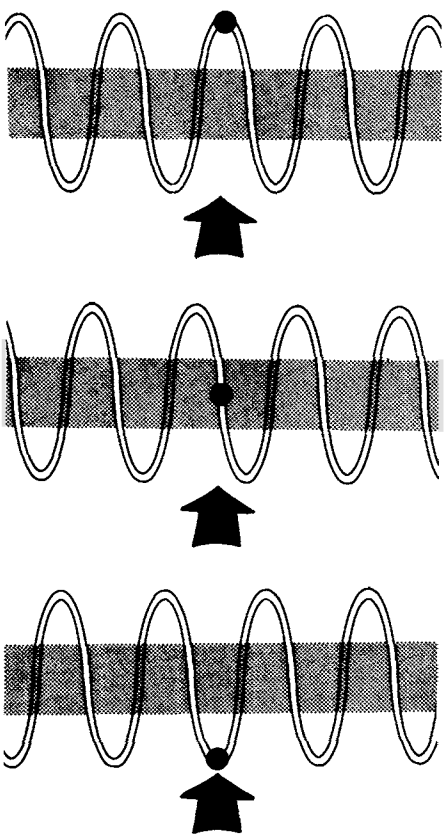

Fig. 9. Model of the rotating spiral flow axis. The sequence shows a rotation of 0, 90, and 180 deg.

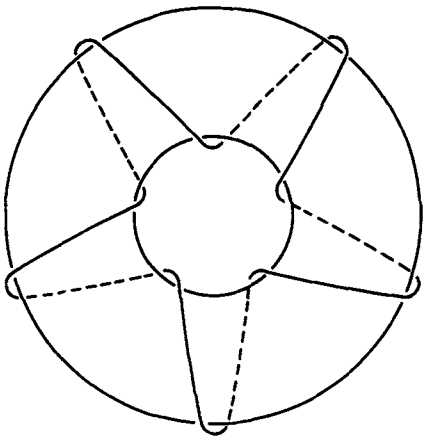

Fig. 10. Sketch of spiral flow axis for mode 3.

CONCLUDING REMARKS

Experimental observations presented here definitely establish the existence of stable oscillatory flows in completely confined fluid layers heated from below. The conditions necessary for the oscillation as well as the qualitative nature of the flow have been explored. These preliminary results provide a framework for more detailed, quantitative measurements; they should also serve as a guide for analytical work.

To recapitulate, experiments were performed with gases heated between horizontal plates, presumed to be at constant temperatures, and laterally confined by vertical cylinders. The cylindrical walls were insulating surfaces (Plexiglas) (although experiments with paper walls and with metal walls gave comparable results). Oscillatory flows were detected in the Rayleigh number range of 20,000 to well over 100,000 with cylinder dimensions of $0.5 < h/R < 2.0$. For the radius greater than twice the height, no oscillations were seen, the flows were irregular, and it appeared that beyond this limit the motion was similar to that in the unbounded layer. Also, it should be noted that previous investigators have reported a transition to turbulence in the infinite layer in the Rayleigh number range in which we detect the oscillatory transition.

Prior to the oscillation, four different modes of flow were observed with the preferred mode depending on the cell dimensions. (Presumably, these modes are established at the first transition to flow—at a Rayleigh number around 2,000; our observations do not extend to the first transition.) At the transition a vortical movement grew out of the basic flow and developed into a stable spiraling motion. It was this spiraling motion which caused the temperature at a point to oscillate. The frequency of the oscillation is a linear function of Rayleigh number and, on a dimensionless basis, the frequency data obtained in all the various cylinders fall into two groups; one group for $(h/R) \geq 1$ and the other for $(h/R) \leq 1$. This grouping is the result of the two categories of convective turnover (types A and B) in which the characteristic dimension of the circulation loop is either the cell radius or the cell diameter.

Several features of the flow depend on the operation of the experiment. Transitions can be induced, or delayed by mechanical and thermal disturbances and they are

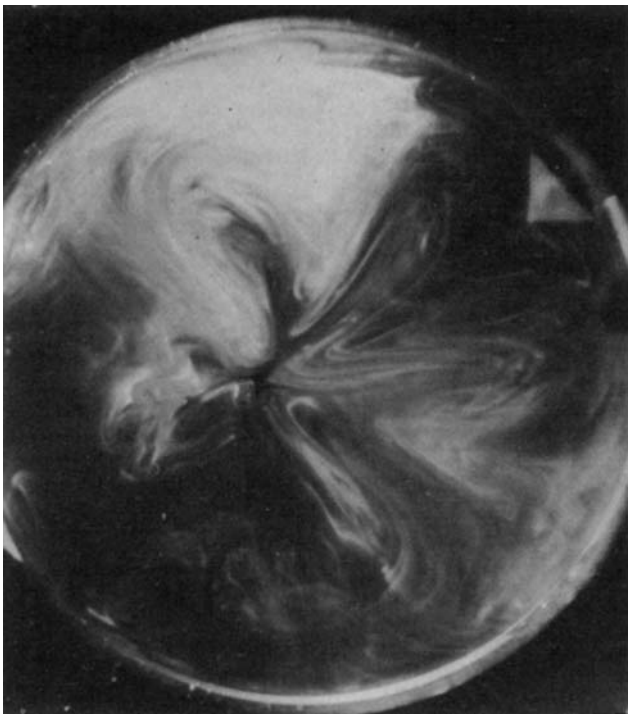

Fig. 11a. Photograph of smoke trace showing oscillatory flow with mode 3. $R = 1.5$ in., $h = 0.8$ in., and $N_{Ra} \sim 65{,}000$.

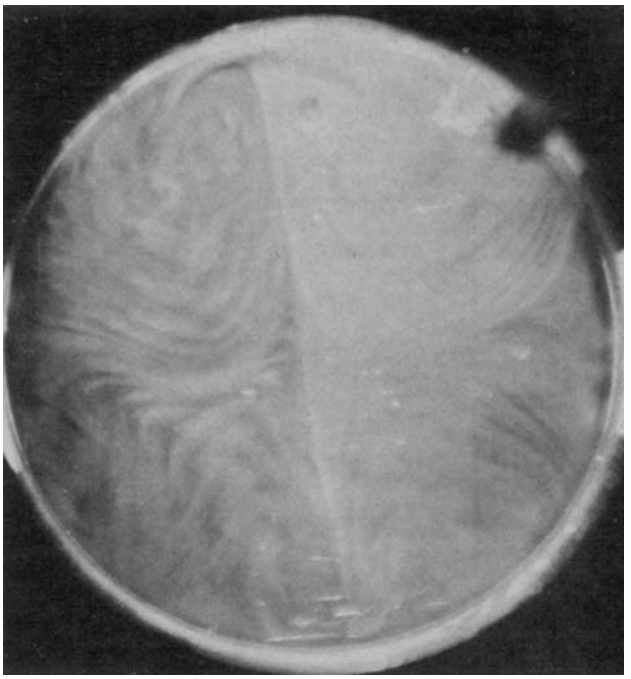

Fig. 11b. Photograph of smoke trace showing flow lines in mode 4 prior to oscillation. $R = 1.24$ in., $h = 0.8$ in., and $N_{Ra} \sim 30{,}000$.

strongly dependent on heating and cooling rates. Flow sequences are not necessarily reversible, for example, a different value was found for the Rayleigh number of a transition depending on whether the value was approached from above or below (in ΔT). Much of the apparent scatter is due to the fact that the various convective states are nearly equivalent in energy, especially at the high Rayleigh numbers.

Convective flow between heated plates is known to be analogous in certain aspects to the flow between rotating cylinders. Recently several experiments have been reported wherein high order transitions have been measured in the rotating cylinder problem (2); also, transitions in Couette flow with a thermal gradient have been examined (15). There may be a connection between these phenomena and the present study; in particular, the transition to turbulence may be similar.

Other recent work which may have bearing on this investigation is the numerical computations of Fromm (3). He has solved numerically the nonlinear equations for a fluid layer heated from below, taking into consideration both periodic (lateral) boundaries and rigid, insulating boundaries. Unfortunately, for present comparisons, Fromm's study is limited to two-dimensional flows. Nevertheless, some interesting results have been observed. For example, he finds an oscillating flow at Rayleigh numbers greater than 10^6. This oscillation has a dimensionless time period $t' = \kappa t/h^2 = 0.010$. The comparable time period for the data of Figure 6 is 0.1, an order of magnitude greater than the numerical result. In addition, Fromm presents calculated isotherms for the bounded case. Examining these isotherms one can readily see how a superimposed rotation might give rise to a very complicated wave form such as measured here.

To answer some of the questions generated by these preliminary observations, further studies are now under way in this laboratory. We are also examining transitions in liquids and though the results are not yet known, it appears that somewhat analogous transitions occur with liquids. These findings will be reported in a future publication.

ACKNOWLEDGMENT

This investigation was supported in part by the U. S. Public Health Service under Research Grant WP-00601. Fellowships received by W. T. Mitchell from the National Science Foundation and from the Minnesota Mining and Manufacturing Company are gratefully acknowledged. Also, the authors are indebted to R. L. Sani for helpful discussions of portions of this work.

NOTATION

a = dimensionless wave number
A_n = arbitrary constant, cm./sec.
f = frequency of temperature oscillation, sec.$^{-1}$
g = acceleration due to gravity, cm./sec.^{2}
h = fluid layer thickness, cm.
J_n = Bessel function of the first kind of order n
k = constant defined by Equation (2), cm.$^{-1}$
N_{Gr} = Grashof number
N_{Pr} = Prandtl number
N_{Ra} = Rayleigh number
r = radial coordinate, cm.
R = radius of circular cell, cm.
ΔT = fixed temperature difference between horizontal plates, °C.
w = velocity component normal to the horizontal plates, cm./sec.

Greek Letters

α = coefficient of volume expansion, °C.$^{-1}$
α_n = arbitrary constant, rad.
θ = angle in cylindrical coordinates, rad.
κ = thermal diffusivity, sq. cm./sec.
ν = kinematic viscosity, sq. cm./sec.

LITERATURE CITED

1. Chandrasekhar, S., "Hydrodynamic and Hydromagnetic Stability," Oxford Univ. Press, London (1961).
2. Coles, D., *J. Fluid Mech.*, **21**, 385 (1965).
3. Fromm, J. E., *Phys. Fluids*, **8**, 1757 (1965).
4. Jeffreys, H., *Proc. Roy. Soc. (London)*, **A118**, 195 (1928).

5. Low, A. R., *ibid.*, **A125**, 180 (1929).
6. Malkus, W. V. R., *ibid.*, **A225**, 185 (1954).
7. Mitchell, W. T., Ph.D. thesis, Univ. Illinois, Urbana (1965).
8. Ostrach, S., and D. Pnueli, *Trans. Am. Soc. Mech. Engrs.*, **85**, 346 (1963).
9. O'Toole, J. L., and P. L. Silveston, *Chem. Engr. Progr. Symposium Ser. No. 32*, **57**, 81 (1961).
10. Pellew, A., and R. V. Southwell, *Proc. Roy. Soc. (London)*, **A176**, 312 (1940).
11. Rayleigh, Lord, *Phil. Mag.*, **32**, 529 (1916); *Sci. Papers*, **6**, 432 (1920).
12. ———, "Theory of Sound," Chap. IX, Macmillan, London (1894).
13. Sani, R. L., and L. E. Scriven, *Phys. Fluids* (to be published).
14. Schmidt, R. J., and O. A. Saunders, *Proc. Roy. Soc. (London)*, **A165**, 216 (1938).
15. Snyder, H. A., and S. K. F. Karlsson, *Phys. Fluids*, **7**, 1696 (1964).
16. Yih, C. S., *Quart. Appl. Math.*, **17**, 25 (1959).

Manuscript received August 13, 1965; revision received April 11, 1966; paper accepted April 18, 1966. Paper presented at A.I.Ch.E. Philadelphia meeting.

Photochlorination in a Tubular Reactor

ALBERTO E. CASSANO and J. M. SMITH

University of California, Davis, California

A method of describing the behavior of a single-phase, photochemical reaction in a tubular flow reactor is given. A simplified form of the equations is applied to experimental data for the chlorination of propane.

The results indicate that the reaction rate is second order in chlorine concentration and first order in light intensity at the wall. Independent experimental actinometer measurements permit the determination of absolute values of the kinetic constants. Such data are rarely available for photochemical reactions. Filter solutions flowing through a jacket around the reactor is shown to be a practical method for studying the effects of light intensity, as well as for cooling the reactor. The optical efficiency of the reactor lamp system was 11%.

The design of photochemical reactors presents a challenging problem because of the interaction of chemical and physical processes. Variations in light intensity and absorption with position can affect the rate of reaction, cause concentration gradients, and induce diffusion. Further, many photochemical reactions are best described by chain mechanisms. For these systems heterogeneous (wall) as well as homogeneous termination steps can occur. If the heterogeneous reaction is significant, diffusion to the reactor wall becomes important. Some of these complications may be eliminated in a stirred-tank (completely mixed) reactor, but this form is seldom plausible for gas phase reactions and may not be advantageous for liquid systems.

The first purpose of this paper is to develop equations for describing the behavior of tubular flow reactors for chain kinetics. The results are complicated, but it is shown that laboratory measurements can be made at conditions which simplify the equations. These latter results are then used to analyze data obtained in a laminar flow reactor for the chlorination of propane at 30°C. and at atmospheric pressure.

The literature includes descriptive reports (*1, 8, 13, 19*) on the scientific and commercial aspects of photoreactors and there are also a few papers on quantitative design. The first of these (*3*) considers the liquid phase reaction between hydrogen sulfide and *n*-octene–1. Backmixing in the flow reactor thwarted a complete analysis of the data. Gaertner and Kent (*11*) studied the photolysis of aqueous uranyl oxalate in an annular reactor. The reaction was of zero order in concentrations, so general conclusions about reactor performance were not possible. Nevertheless, the work confirmed the use of the uranyl sulfate reaction for measurement of light intensity. Schechter and Wissler (*24*) studied theoretically the performance of a laminar flow reactor. They included the effects of diffusion, convection, and light attenuation but used simple kinetics (nonchain reaction) and assumed a constant attenuation coefficient. A valuable contribution of their paper is the sound treatment of the boundary condition at the center of the tube.

Huff and Walker (*17*) reported on the photochlorination of chloroform in a tubular reactor. Their interpretation, while neglecting diffusion and flow effects, apparently represents the first contribution to reactor design for a chain reaction. There are two contributions of Dranoff and colleagues which attack the design problem for simple, nonchain kinetics. The first (*15*) includes equations for a completely mixed reactor with application to data on the photodecomposition of chloroplatinic acid. The second (*9*) considers the more important tubular flow reactor with the use of dimensional analysis. For simple reactions this approach can be useful for the scale-up of some parameters in the system. For chain reactions equations are obtained which are not practical for analysis and are probably not practical for scaling up as well. While these initial contributions are valuable, more work needs to be done both experimentally and theoretically in order to be able to analyze and to predict reactor behavior, particularly for chain reactions.

The chlorination of propane was chosen for the experimental measurements because the evidence (*21* to *23, 25,*

Alberto E. Cassano is on leave from the Facultad de Ingenieria Quimica, Santa Fe, Argentina.